Coherent Four-Wave Mixing on Hybrid Graphene-Silicon Photonic Crystals

Tingyi Gu, Hao Zhou, James F. McMillan, Nicholas Petrone, Arend van der Zande, James C. Hone, Mingbin Yu, Guo-Qiang Lo, Dim-Lee Kwong, *Fellow, IEEE*, and Chee Wei Wong

(Invited Paper)

***Abstract*—By placing monolayer graphene on silicon membrane, the effective Kerr coefficient of the hybrid media is enhanced 20 times compared to monolithic silicon. Optical four-wave mixing in graphene-silicon photonic crystal waveguide and a single mode cavity are observed at sub-milliwatt continuous wave input. This allows nonlinear functionalities including low power switching/gating, signal regeneration and parametric conversion, enhancing CMOS integrated photonic information processing on chips.**

***Index Terms*—Four-wave mixing, graphene optoelectronics, photonic crystals.**

I. Introduction

THE optical Kerr effect is one of non-resonant electronic nonlinear polarizabilities. It occurs as the result of the nonlinear response of bound electrons to an applied optical field [1]. Third-order nonlinearity susceptibility for graphene is reported as large as $|\chi^{(3)}|\sim 10^{-7}$ esu in IR and mid-IR range, verified by coherent four-wave mixing and third harmonic generation [2]–[5]. Four-wave mixing can be viewed as the elastic scattering of two photons of a high power pump beam, which results in the generation of two new photons at different frequencies. For turning the exceptional nonlinear properties of graphene into functional devices, extended work on integrating graphene into conventional photonic platform has been shown [5]. Here we show the experimental demonstration of high third-order nonlinear response of graphene integrated photonic crystal devices including slow-light waveguides and resonant cavities, and theoretical calculation for predicting the effective nonlinear coefficient of the hybrid optical components.

Manuscript received August 5, 2013; revised October 14, 2013; accepted October 28, 2013. Date of publication December 13, 2013; date of current version January 2, 2014.

T. Gu, J. F. McMillan, and C. W. Wong are with the Optical Nanostructures Laboratory, Center for Integrated Science and Engineering, Solid-State Science and Engineering, and Mechanical Engineering, Columbia University, New York, NY 10027 USA (e-mail: tg2342@columbia.edu; jfm2113@columbia.edu; cww2104@columbia.edu).

H. Zhou is with the Optical Nanostructures Laboratory, Center for Integrated Science and Engineering, Solid-State Science and Engineering, and Mechanical Engineering, Columbia University, New York, NY 10027 and also with the College of Electronic Information, Sichuan University, Chengdu 610064, China (e-mail: hz2299@columbia.edu).

N. Petrone, A. van der Zande, and J. C. Hone, are with the Mechanical Engineering, Columbia University, New York, NY 10027 USA (e-mail: nwp2105@columbia.edu; av2466@columbia.edu; jh2228@columbia.edu).

M. Yu, G.-Q. Lo, and D.-L. Kwong are with the Institute of Microelectronics, Singapore, Singapore 117685 (e-mail: mingbin@ime.a-star.edu.sg; logq@ime.a-star.edu.sg; kwongdl@ime.a-star.edu.sg).

Color versions of one or more of the figures in this paper are available online at http://ieeexplore.ieee.org.

Digital Object Identifier 10.1109/JSTQE.2013.2290274

II. Kerr Coefficient in Graphene

In non-parabolic graphene, the induced nonlinear current is obtained in Ref. [2] by solution of the quantum kinetic equation: $(i\hbar)\partial\rho/\partial t = [\hat{H}, \rho]$, with the Hamiltonian: $\hat{H}=\hat{H}_o + exp(E_1\ cos\omega_1\ t + E_2\ cos\ \omega_2\ t)$ where E_1 and E_1 are the two external field amplitudes with frequencies ω_1 (pump) and ω_2 (signal) incident on graphene. The resulting amplitude of sheet current generated at the harmonics frequencies $(2\omega_1 - \omega_2)$ is described by [2], [5]:

$$j_e = -\frac{3}{32}\frac{e^2}{\hbar}\varepsilon_2\left(\frac{ev_F\varepsilon_1}{\hbar\omega_1\omega_2}\right)^2\frac{2\omega_1^2+2\omega_1\omega_2-\omega_2^2}{\omega_1\left(2\omega_1-\omega_2\right)} \tag{1}$$

where ε_1 and ε_2 are the electric field amplitudes of the incident light at frequencies ω_1 and ω_2 respectively. v_F ($= 10^6$ m/s) is the Fermi velocity of graphene. Under the condition that both ω_1 and ω_2 are close to ω, the sheet conductivity can be approximated as:

$$\sigma^{(3)} = \frac{j_e}{\varepsilon_1\varepsilon_1\varepsilon_2} = -\frac{9}{32}\frac{e^2}{\hbar}\left(\frac{ev_F}{\hbar\omega^2}\right)^2. \tag{2}$$

Since most of the sheet current is generated in graphene, the effective nonlinear susceptibility of the whole membrane can be expressed as:

$$X^{(3)} = \frac{\sigma^{(3)}}{\omega d} = -\frac{9}{32}\frac{e^4v_F^2}{\hbar^3c^5}\frac{\lambda^5}{d} \tag{3}$$

where d is the thickness of the graphene ($\sim$1 nm), λ is the wavelength, and c is the speed of light in vacuum. The calculated $\chi^{(3)}$ of a monolayer graphene is in the order of 10^{-7} esu [corresponding to a Kerr coefficient $n_2 \sim 10^{-13}$m^2/W; $n_2 = 3\chi^{(3)}/(4\ c\varepsilon)$], at 10^5 times higher than in silicon [6] ($\chi^{(3)} \sim 10^{-13}$esu, $n_2 \sim 3.8\times10^{-18}$m^2/W).

III. Dynamic Conductivity in Graphene

Effective n_2 depends on the spatial distribution of optical mode. In order to rigorously calculate the spatial field distribution. We firstly derive the permittivity and effective refractive index of graphene based on the incident photon energy and the Fermi level of graphene. The dynamic conductivity for intra- and inter-band optical transitions [7] can be determined from the Kubo formalism as [8], [5]:

$$\sigma_{\text{intra}}(\omega) = \frac{je^2\mu}{\pi\hbar(\omega + j\tau^{-1})} \tag{4.1}$$

$$\sigma_{\text{inter}}(\omega) = \frac{je^2\mu}{4\pi\hbar}\ln\left(\frac{2\left|\mu\right| - \hbar\left(\omega + j\tau^{-1}\right)}{2\left|\mu\right| + \hbar\left(\omega + j\tau^{-1}\right)}\right) \tag{4.2}$$

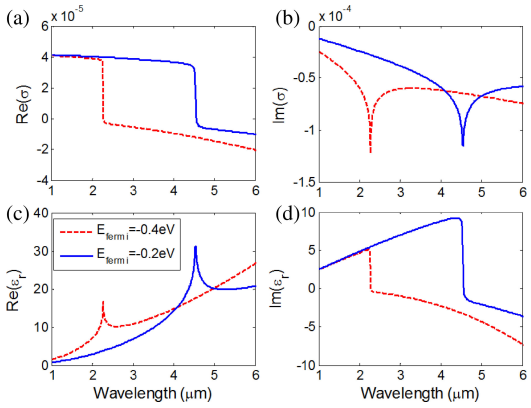

Fig. 1. Conductivity and permittivity of graphene in the IR range. (a) and (b), The real and imaginary parts of the total conductivity. (c) and (d), permittivity, with Fermi level set at – 0.4 eV (red dashed line) and – 0.2 eV (blue solid line), respectively.

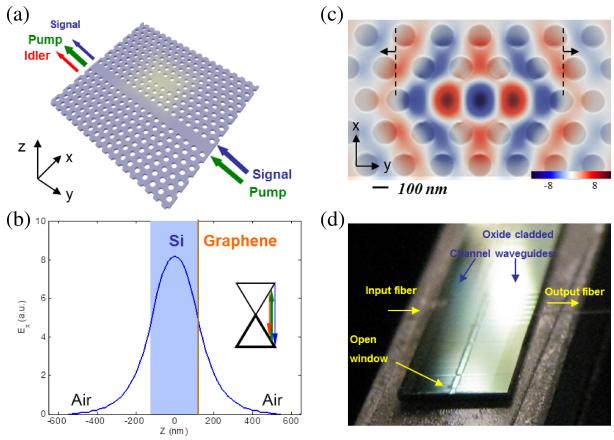

Fig. 2. Device layout and measurement. (a), Structure schematic of an $L3$ cavity switch formed in graphene cladded silicon membrane. (b) Electric field distribution along z direction simulated by FDTD method. The graphene sheet (brown line) is placed on 250 nm thick silicon membrane. Inset: Schematics of graphene band diagram with photon energy of pump (green), and converted ones (red and blue). (c) Top view of optic field energy distribution of an isolated S_1-shifted $L3$ cavity. The FDTD simulation of mode profile is superimposed on the SEM picture S_1-shifted $L3$ cavity with graphene cladding, with mode volume: 0.073 μm^3, and quality factor ~2.0×10^4 Scale bar: 100 nm. (d) CMOS processed integrated optical devices under test. The open window is for silicon membrane undercut and graphene cladding on the photonic crystal part.

where e is the electron charge, $\hbar$ is the reduced Plank constant, ω is the radian frequency, μ is chemical potential, and τ is the relaxation time (1.2 ps for interband conductivity and 100 fs for intraband conductivity). The dynamic conductivity of intra- and inter-band transitions at 1560 nm are (–0.07–0.90i)$\times10^{-5}$ and (4.15–0.95i)$\times10^{-5}$ respectively, leading to the total dynamic conductivity $\sigma_{total} = \sigma_{intra} + \sigma_{inter}$ of (4.1–1.8i)$\times10^{-5}$. The real and imaginary parts of the conductivity and permittivity are calculated in Fig. 1. Given negative imaginary part of total conductivity, the TE mode is supported in graphene [8]. The light can travel along the graphene sheet with weak damping and thus no significant loss is observed for the quasi-TE mode confined in the cavity [9]. The Fermi level in CVD grown graphene is determined by the chemical doping level, about -0.2eV, correspondent to the red dashed curves in Fig. 1.

IV. Modeling Effective Kerr Coefficient in Graphene-Silicon Structures

The structure examined is a hybrid graphene-silicon cavity, achieved by transfer of monolayer large-area graphene sheet onto air-bridged silicon photonic crystal nanomembranes, with minimal linear absorption and optimized optical input/output coupling. Fig. 2(a) shows the device layout, with the input pump and signal lasers and additional output idler. The optical field distribution and confinement in cavity are shown in Fig. 2(b). From cross-section image, the electromagnetic field overlaps with the monolayer graphene at the top [see Fig. 2(c)]. We note that this study is complemented with recent examinations of large-area [10], [11] graphene field-effect transistors and analog circuit designs [12] for potential large-scale silicon integration [see Fig. 2(d)].

Effective n_2 of the hybrid graphene-silicon cavity is then calculated for an inhomogeneous cross-section weighted with respect to field distribution [13] [see Fig. 3(a)–(f)]. The 3D FDTD method with sub-pixel averaging is used to calculate the real and imaginary parts of the E-field distribution for the cavity resonant mode. The spatial resolution is set at 1/30 of the lattice constant (14 nm). Time-domain coupled mode theory, including free carrier dispersion and dynamics and thermal time constants, is carried out with 1 ps temporal resolution.

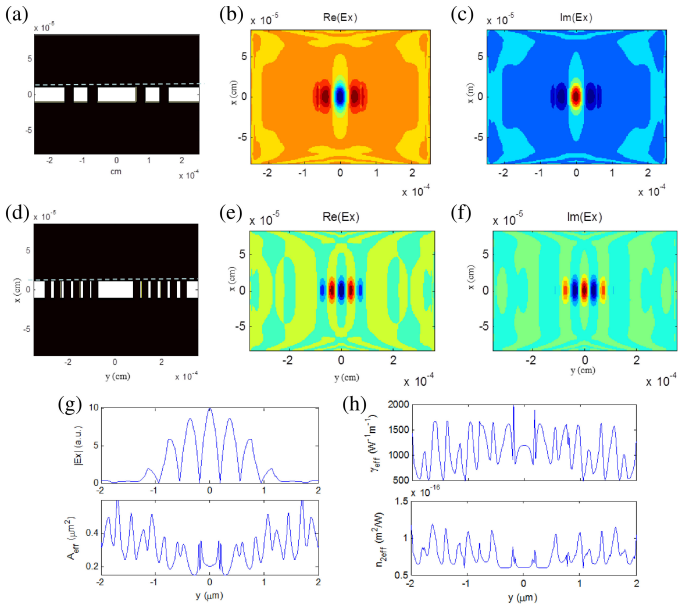

Fig. 3. Optical field distribution and calculation for effective Kerr nonlinearity of the hybrid graphene-silicon waveguide. (a), The refractive index on the $x = 0$ plane. The white part is the silicon ($n = 3.45$) and the dark part is the air ($n = 1$), (b) and (c), real and imaginary parts of TE polarized electric field distribution on the across section in (a), (d), The refractive index on the $y = 0$ plane. (e) and (f), real and imaginary parts of TE polarized electric field in (d). (g), The amplitude of electric field along the cross section of waveguide (up), and effective area (down) along the waveguide direction. (h), nonlinear parameter γ ($= \omega n_2 / c A_{\text{eff}}$) and effective Kerr coefficient of graphene silicon waveguide.

TABLE I
FIELD-BALANCED CALCULATED KERR COEFFICIENTS

Computed parameters	$\overline{n_2}$ (m^2/W)
Graphene	10^{-13} [6]
Silicon	3.8×10^{-18}
Monolayer graphene-silicon	7.7×10^{-17}
Chalcogenide waveguide	7.0×10^{-17}

With a baseline model without complex graphene-silicon electronic interactions, the effective n_2 can be expressed as:

$$\begin{aligned}\overline{n_2} &= \left(\frac{\lambda_0}{2\pi}\right)^d \frac{\int n^2(r)n_2(r)(|E(r)\cdot E(r)|^2 + 2|E(r)\cdot E(r)^*|^2)d^dr}{(\int n^2(r)|E(r)|^2 d^dr)^2} \\ &= \left(\frac{\lambda_0}{2\pi}\right)^d \frac{n_{Si}^2 n_{2Si}\int_{Si}(|E(r)\cdot E(r)|^2 + 2|E(r)\cdot E(r)^*|^2)d^dr}{(\int n^2(r)|E(r)|^2 d^dr)^2} \\ &\quad + \left(\frac{\lambda_0}{2\pi}\right)^d \frac{n_{Gr}^2 n_{2Gr}\int_{Gr}(|E(r)\cdot E(r)|^2 + 2|E(r)\cdot E(r)^*|^2)d^dr}{(\int n^2(r)|E(r)|^2 d^dr)^2} \\ &= (3.8 + 73.2)\times 10^{-18} = 7.7\times 10^{-17} \end{aligned} \quad (5)$$

where *E(r)* is the complex fields in the cavity. λ_0 is the wavelength in vacuum, and $d = 3$ is the number of dimensions. The complex electric field *E(r)* is obtained from Three-dimensional finite-difference time-domain computations of the optical cavity examined [14]. *n(r)* is the local refractive index. The local Kerr coefficient $n_2(r)$ is 3.8×10^{-18}m^2/W in silicon membrane and $\sim10^{-13}$m^2/W for graphene. Both *n(r)* and $n_2(r)$ are homogeneous in silicon and graphene, so the total effective n_2 can be decomposed into two components for graphene and silicon separately.

The resulting field-balanced effective n_2 is calculated to be 7.7×10^{-17}m^2/W ($\chi^{(3)}\sim 10^{-12}$ esu) as shown in the below Table I [5], close to the best reported chalcogenide photonic crystal waveguides [15], [16].

The resulting nonlinear parameter γ ($=\omega n_2/cA_{\text{eff}}$) is derived to be 800 W^{-1}m^{-1}, for an effective mode area of 0.25 μm^2.

V. OBSERVATIONS OF FOUR-WAVE MIXING IN PHOTONIC CRYSTAL WAVEGUIDE AND CAVITY

A. Hybrid Photonic Crystal Waveguide

To examine only the Kerr nonlinearity, next we performed degenerate four-wave mixing measurements on the hybrid graphene–silicon photonic crystal waveguide, with continuous-wave laser input. In photonic crystal waveguide, the FWM parametric gain coefficient is defined as $g = [\gamma^* \overline{P}_{\text{pump}}\Delta k - (\Delta k/2)^2]^{1/2}$. The signal-to-idler conversion efficiency (CE) is given by [17]:

$$G_{\text{idler}} = \frac{P_{\text{idler}}^{\text{out}}}{P_{\text{signal}}^{\text{in}}} = \left(\gamma^0 L_e\right)^2 S^4 e^{-\alpha_{\text{idler}} S L_e} \quad (6)$$

where $\gamma = \omega n_2/cA_{\text{eff}}$, is the effective third order nonlinear parameter in waveguide. The effective mode area (A_{eff}) of the PhC waveguide mode is calculated to be around 0.25 μm^2.

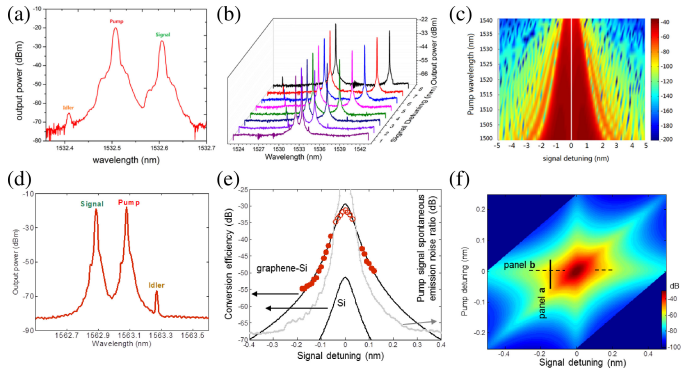

Fig. 4. Measurement of four-wave mixing in graphene-silicon PhC structures. (a), Output spectrum of W1 PhCWG with graphene. Pump wavelength is set at 1532.5 nm, signal detuning is set at +100 pm. (b), Measured CE versus signal detuning from +1 nm to +8 nm with pump wavelength fixed at ~ 1532.5 nm. (c), Simulation of the four-wave mixing in PhCWG with graphene. The signal laser is detuned from pump wavelength from – 4 nm to + 4 nm, and pump from 1500 nm to 1540 nm. (d), Output spectrum of *L*3 cavity. Signal detuning is set at -150 pm, and pump is set on cavity resonance. (e), Measured CE versus signal detuning, with pump power set on cavity resonance. Inset: Conversion efficiency versus pump detuning from the cavity resonance. (f), Mapping the four-wave mixing in the single cavity with different signal detuning. The pump laser is set on resonance of the cavity and enhanced by the cavity resonance. The signal laser is detuned from cavity resonance from 70 pm to 200 pm [5].

The pump power is from a continuous-wave tunable laser near 1535 nm, and amplified by EDFA. The highest measured CE is about -37 dB. Linear absorption increases from 0.05 dB/um to 0.15 dB/um after transferring graphene in this case. The waveguide we used here is 200 um long (L_e). In this sample, the CE is almost the same as compared to the same geometry without graphene because graphene induces both the higher n_2 and the higher α_{idler} mentioned in equation (6). We derived the CE versus pump and probe detunings. Experimental measurements and theoretical predictions are shown in Fig. 4(a)–(c). Considering the trade-off between the linear absorption and conversion efficiency, the optimized length of the graphene waveguide for achieving the best CE is L_e around 60 micrometers for this graphene linear absorption level.

B. Hybrid Photonic Crystal Cavity

For the microcavity four-wave mixing, a relatively modest Q of 7,500 was chosen to allow a $\sim$ 200 pm cavity linewidth within which the highly dispersive four-wave mixing can be examined. The input pump and signal laser detunings are placed within this linewidth, with matched TE-like input polarization, and the powers set at 600 μW. Two example series of idler measurements are illustrated in Fig. 4(d)–(e), with differential pump and signal detunings respectively. In both series the parametric idler is clearly observed as a sideband to the cavity resonance, with the pump detuning ranging -100 pm to 30 pm and the signal detuning shown in Fig. 4(e). For each fixed signal- and pump-cavity detunings, the generated idler shows a slight intensity roll-off from linear signal (or pump) power dependence when the transmitted signal (or pump) power is greater than $\sim$ 400 μW due to increasing free-carrier absorption effects.

The CE of the single cavity $\eta = |\gamma P_p L'|^2 \mathrm{FE}_p^4 \mathrm{FE}_s{}^2 \mathrm{FE}_c{}^2$, where FE_p, FE_s, and FE_c are the field enhancement factors of pump, signal and idler respectively [18]. The effective length L' includes the phase mismatch and loss effects. Compared to the original cavity length ($\sim$ 1582.6 nm), the effective cavity length is only slightly modified by less than 1 nm. However, the spectral dependent field enhancement factor is the square of the cavity build-up factor $\mathrm{FE}^2 = \mathrm{P_{cav}/P_{wg}} = \mathrm{F(U/U_{max})}\eta_p{}^2$, where $\mathrm{U/U_{max}}$ is the normalized energy distribution with the Lorentzian lineshape. $\eta_p = 0.33$ is the correction term for the spatial misalignment between the quasi-TE mode and graphene, and the optical field polarization. The field enhancement effect in the cavity is proportional to the photon mode density: $F = Q\lambda^3/(8\pi V)$ [19], where Q is the total quality factor, λ is the wavelength of the light, and V is the cavity mode volume.

The enhanced two-photon-absorption and induced free-carrier absorption would produce nonlinear losses. To investigate the direct effect of two-photon absorption and free-carrier absorption on the four-wave mixing, we measure the CE with varying input signal power. Extra 4-dB loss is measured when the input signal power increases from -22 to -10 dBm, with the additional contribution from nonlinear absorption of the graphene-silicon cavity membrane.

A theoretical four-wave mixing model with cavity field enhancement [Fig. 4(e)–(f)] matches with these first graphene-cavity observations. The detuning between the cavity resonance and the laser would decrease the field enhancement factor:

$$F(\lambda) = F(\lambda_{\mathrm{cav}}) \frac{1}{1 + 4Q^2 \left(\frac{\lambda}{\lambda_{\mathrm{cav}}} - 1\right)^2}. \tag{7}$$

Based on this numerical model match to the experimental observations, the observed Kerr coefficient n_2 of the graphene-silicon cavity ensemble is $4.8\times10^{-17}\mathrm{m}^2/\mathrm{W}$, an order of magnitude larger than in monolithic silicon and GaInP-related materials [12], and two orders of magnitude larger than in silicon nitride [20]. The computed n_2 is at $7.7\times10^{-17}\mathrm{m}^2/\mathrm{W}$, in the same order of magnitude as the observed four-wave mixing derived n_2. The remaining discrepancies arise from a Fermi velocity slightly smaller than the ideal values ($\sim 10^6$ m/s) in the graphene. As illustrated in Fig. 4(e) for both measurement and theory, the derived conversion efficiencies are observed up to -30-dB in the un-optimized graphene-cavity, even at cavity Qs of 7,500 and low pump powers of 600 μW. We note that for a silicon cavity without graphene the conversion efficiencies are dramatically lower [dashed grey line in Fig. 4(e)], and even below the pump/signal laser spontaneous emission noise ratio preventing observation of four-wave mixing in a single monolithic silicon photonic crystal cavity until now.

VI. Conclusion

Graphene contributes 95% to the effective Kerr coefficient of the hybrid graphene-silicon media and, with large doping, only adds slightly to the linear absorption. These observations, in comparison with control measurements on solely monolithic silicon photonic crystal waveguides and cavities, are enabled only by the dramatically-large $\chi^{(3)}$ nonlinearities in graphene and the large Q/V ratios in wavelength-localized photonic crystal cavities. These nonlinear results demonstrate the feasibility and versatility of hybrid two-dimensional graphene-silicon nanophotonic devices for next-generation chip-scale radio-frequency light source and optical modulator for all-optical signal processing.

References

[1] R. W. Boyd, *Nonlinear Optics*. New York, NY, USA: Academic Press, 2002.

[2] E. Hendry, P. J. Hale, J. Moger, and A. K. Savchenko, "Coherent nonlinear optical response of graphene," *Phys. Rev. Lett.*, vol. 105, p. 097401, 2010.

[3] N. Kumar, J. Kumar, C. Gerstenkorn, R. Wang, H.-Y. Chiu, A. L. Smirl, and H. Zhao, "Third harmonic generation in graphene and few-layer graphite films," *Phys. Rev.*, vol. B 87, p. 121406, 2013.

[4] S.-Y. Hong, J. I. Dadap, N. Petrone, P.-C. Yeh, J. Hone, and R. M. Osgood Jr., "Optical third-harmonic generation in graphene," *Phys. Rev. X 3*, vol. 3, p. 021014, 2013.

[5] T. Gu, N. Petrone, J. F. McMillan, A. van der Zande, M. Yu, G.-Q. Lo, D. L. Kwong, J. Hone, and C. W. Wong, "Regenerative oscillation and four-wave mixing in graphene optoelectronics," *Nature Photon.*, vol. 6, pp. 554–559, 2012.

[6] M. Dinu, F. Quochi, and H. Garcia, "Third-order nonlinearities in silicon at telecom wavelengths," *Appl. Phys. Lett.*, vol. 82, p. 2954, 2003.

[7] K. F. Mak, M. Y. Sfeir, Y. Wu, C. H. Lui, J. A. Misewich, and T. F. Heinz, "Measurement of the optical conductivity of graphene," *Phys. Rev. Lett.*, vol. 101, p. 196405, 2008.

[8] Q. Bao, H. Zhang, B. Wang, Z. Ni, C. H. Y. X. Lim, Y. Wang, D. Yuan Tang, and K. P. Loh, "Broadband graphene polarizer," *Nature Photon.*, vol. 5, pp. 411–415, 2011.

[9] S. Mikhailov and K. Ziegler, "New electromagnetic mode in graphene," *Phys. Rev. Lett.*, vol. 99, p. 016803, 2007.

[10] F. Morichetti, A. Canciamilla, C. Ferrari, A. Samarelli, M. Sorel, and A. Melloni, "Travelling-wave resonant four-wave mixing breaks the limits of cavity-enhanced all-optical wavelength conversion," *Nature Commun.*, vol. 2, p. 296, 2011.

[11] M. A. Foster, R. Salem, D. F. Geraghty, A. C. Turner-Foster, M. Lipson, and A. L. Gaeta, "Silicon-chip-based ultrafast optical oscilloscope," *Nature*, vol. 456, pp. 81–84, 2008.

[12] A. Pasquazi, M. Peccianti, Y. Park, B. E. Little, S. T. Chu, R. Morandotti, J. Azaña, and D. J. Moss, "Sub-picosecond phase-sensitive optical pulse characterization on a chip," *Nature Photon.*, vol. 5, pp. 618–623, 2011.

[13] S. Afshar V. and T. M. Monro, "A full vectorial model for pulse propagation in emerging waveguides with subwavelength structures part I: Kerr nonlinearity," *Opt. Exp.*, vol. 17, pp. 2298–2318, 2009.

[14] A. F. Oskooi, D. Roundy, M. Ibanescu, P. Bermel, J. D. Joannopoulos, and S. G. Johnson, "MEEP: A flexible free-software package for electromagnetic simulations by the FDTD method," *Comput. Phys. Commun.*, vol. 181, pp. 687–702, 2010.

[15] B. J. Eggleton, B. Luther-Davies, and K. Richardson, "Chalcogenide photonics," *Nature Photon.*, vol. 5, pp. 141–148, 2011.

[16] K. Suzuki, Y. Hamachi, and T. Baba, "Fabrication and characterization of chalcogenide glass photonic crystal waveguides," *Opt. Exp.*, vol. 17, pp. 22393–22400, 2009.

[17] J. F. McMillan, M. Yu, D.-L. Kwong, and C. W. Wong, "Observations of four-wave mixing in slow-light silicon photonic crystal waveguides," *Opt. Exp.*, vol. 18, pp. 15484–15497, 2010.

[18] P. P. Absil, J. V. Hryniewicz, B. E. Little, P. S. Cho, R. A. Wilson, L. G. Joneckis, and P.-T. Ho, "Wavelength conversion in GaAs micro-ring resonators," *Opt. Lett.*, vol. 25, pp. 554–556, 2000.

[19] R. K. Chang and A. J. Campillo, *Optical Processes in Microcavities*. Singapore: World Scientific, 1996.

[20] F. Wang, Y. Zhang, C. Tian, C. Girit, A. Zettl, M. Crommie, and Y. R. Shen, "Gate-variable optical transitions in graphene," *Science*, vol. 320, pp. 206–209, 2008.

Tingyi Gu received the B.Eng. degree in information technology from Shanghai Jiaotong University, Shanghai, China, in 2008, and the M.Sc. degree in electrical engineering from Columbia University, New York, NY, USA, in 2010. She was at the Center for High Technology, University of New Mexico, Albuquerque, NM, USA, about one year and half on photoluminescence of colloidal quantum dots optical calibration and carrier migration in the InAs quantum dots solar cells. She is currently working toward the Ph.D. degree at Columbia University, in the optical nanostructure laboratory. Her current research focuses on understanding the optoelectronic properties of semiconductor in nanostructured devices, as well as wiring them to implementation in integrated photonic circuits.

Hao Zhou received the B.S. degree in science and technology of optical information in Sichuan University, Chengdu, China, in 2008. He is currently a doctoral candidate in optical engineering in Sichuan University and a visiting student in Optical Nanostructures Laboratory in Columbia University, New York, NY, USA, with the interest of graphene devices.

James F. McMillan received the B.A.Sc. degree in electrical engineering from the University of Toronto, Toronto, ON, Canada, in 2004, and the M.S. degree in 2006 from Columbia University, New York, NY, USA, where he is currently working toward the Ph.D. degree. His current research interests include photonic crystal waveguides and slow-light enhancement of light-matter interaction.

Nicholas Petrone received the B.S. degree in mechanical engineering from Johns Hopkins University, Baltimore, MD, USA, in 2005 and the M.S. degree in mechanical engineering from the University of California, Los Angeles, CA, USA, in 2008. Since 2008, he has been working toward the Ph.D. degree in the Department of Mechanical Engineering at Columbia University, New York, NY, USA. His research interests include the synthesis of large-area films of graphene by chemical vapor deposition as well as the fabrication and characterization of graphene-based flexible electronics, such as radio-frequency field-effect transistors and transparent conductive electrodes. Mr. petrone is a member of Pi Tau Sigma, the American Society of Mechanical Engineers, the American Physical Society, and the Materials Research Society.

Arend van der Zande is an expert in the synthesis of novel 2-D materials and uses them to fabricate new, highly tunable optoelecronic and mechanical devices. He is a Postdoctoral Fellow at the Columbia University Energy Frontier Research Center. He received the the Master's degree in 2009 and the Ph.D. degree in 2011, both from Cornell University, Ithaca, NY, USA. From 1999 to 2003, he received the double degree, in physics and mathematics from the University of California, Santa Cruz, CA, USA. He has published 20 + journal papers and delivered more than ten invited talks at universities and industry. Dr. van der Zande received two patents and has two provisional patents currently. His work has appeared in *Nature*, *Nature Materials*, *Science*, *Nature Photonics*, and *Nano Letters*, among others.

James C. Hone received the B.S. degree in physics from Yale University, New Haven, CT, USA, in 1990, and the M.S. and Ph.D degrees in physics from the University of California, Berkeley, CA, USA, in 1994 and 1998, respectively. He is currently a Professor of mechanical engineering at Columbia University, New York, NY, USA. His research interests include carbon nanotubes, graphene and other layered materials, and nanobiology.

Mingbin Yu is a Member of the Technical Staff at the Institute of Microelectronics in Singapore. For contributions in advancing semiconductor technology and industry development through leading edge research on silicon photonics, he received the 2010 President's Technology Award, together with Dr. Guo-Qiang Lo, Dr. Kah Wee Ang, and Dr. Tsung-Yang Liow of the Institute of Microelectronics, A∗STAR. The team also received the 2011 IES Prestigious Engineer Achievement Award for high-performance silicon photonics and plasmonics. The team has published more than 50 papers in top prestigious journals, leading IME to earn a reputation as a world leading cost-effective solutions provider for ultrahigh data-rate low-cost optical communications.

Guo-Qiang Lo received the M.S. and Ph.D. degrees in electrical and computer engineering from the University of Texas at Austin, Austin, TX, USA, in 1989 and 1992, respectively. Before he came to Singapore, for 12 years, he was with Integrated Device Technology, Inc., in both San Jose, CA, USA, and Hillsboro. OR: working on Si semiconductor manufacturing areas in process and integration module research and development. Since 2004, he has been with IME, Singapore. He is currently the Deputy Executive Director for RD in IME, and also Program Directors for Photonics/Electronics. He is an author or coauthor of more than 100 peer-reviewed journal and conferences publications, and more than 20 granted U.S. patents. His RD interests are in novel semiconductor device and integration technology, particularly in nanoelectronics devices and Si-micro-photonics. Dr. Lo received the IEEE George E. Smith Award in 2008 for Best Paper Published in IEEE ELECTRONIC DEVICE LETTERS in 2007. In addition, he has won NTA/Singapore in 2008 and PTA/Singapore in 2010 for Electronics and Photonics, respectively.

Dim-Lee Kwong is the Executive Director of Institute of Microelectronics, Agency for Science, Technology and Research (A∗STAR), Singapore and a Professor of Electrical and Computer Engineering at the National University of Singapore, Singapore. He was a Earl N. and Margaret Bransfield Endowed Professor of Electrical and Computer Engineering at The University of Texas at Austin, Austin, TX, USA, from 1990 to 2007 and the Temasek Professor of National University of Singapore from 2001–2004. Prof. Kwong received the IBM Faculty Award in 1984 – 1986, Semiconductor Research Corporation (SRC) Inventor Awards in 1993 – 1994, General Motor Foundation Fellowship in 1992–1995, Halliburton Foundation Excellent Teaching Award in 1994, Engineering Foundation Award in 1995, IEEE George Smith Award in 2007, and the 2011 IEEE Frederik Philips Award with citation: "*For leadership in silicon technology and excellence in the management of microelectronics R&D*." He is a Fellow of the IEEE, is the author of more than 1100 referred archival publications (610 journal and 510 conference proceedings), has presented more than 90 plenary and invited talks at international conferences, and has been awarded with more than 25 U.S. patents. More than 60 students received their Ph.D. degrees under his supervision.

Chee Wei Wong advances the control of photons in mesoscopic systems, involving nonlinear, ultrafast, quantum and precision measurements. He is a Faculty Member with Columbia University in the Center for Integrated Science and Engineering, Solid-State Science and Engineering, and Mechanical Engineering, since 2004. Dr. Wei Wong received the DARPA Young Faculty Award in 2007, the NSF CAREER Award in 2008, the 3M Faculty Award in 2009, and elected a Fellow of the Optical Society of America in 2013. He received the Sc.D. degree in 2003 and the S.M. degree in 2001, both from the Massachusetts Institute of Technology, Cambridge, MA, USA. From 1999 to 1996, he received the double degree, B. Sc. highest honors and B.A. highest honors, both at the University of California at Berkeley. Since 2003, he has been published four book chapters, 70+ journal papers, and 100+ conference articles, and has delivered 60+ invited talks at universities and industry. He has recived 10 patents and has 12 provisional patents currently. His work has appeared in *Nature*, *Nature Communications*, *Nature Photonics*, *Scientific Reports*, *Physical Review Letters*, *Nano Letters*, among others.